Inorganica Chimica Acta xxx (2014) xxx–xxx

Contents lists available at ScienceDirect

Inorganica Chimica Acta

journal homepage: www.elsevier.com/locate/ica

Synthesis, characterization and cytotoxic activity studies of two ruthenium(II) complexes

Wei Li [a], Bing-Jie Han [a], Ji Wang [a], Guang-Bin Jiang [a], Yang-Yin Xie [a], Gan-Jian Lin [a], Hong-Liang Huang [b,*], Yun-Jun Liu [a,*]

[a] School of Pharmacy, Guangdong Pharmaceutical University, Guangzhou 510006, PR China
[b] School of Life Science and Biopharmaceutical, Guangdong Pharmaceutical University, Guangzhou 510006, PR China

ARTICLE INFO

Article history:
Received 25 April 2014
Received in revised form 10 July 2014
Accepted 11 July 2014
Available online xxxx

SI: Antitumor Active Organotin Compounds

Keywords:
Ru(II) complexes
Cytotoxicity in vitro
Apoptosis
ROS
Mitochondrial membrane potential
Cell cycle arrest

ABSTRACT

Two Ru(II) polypyridyl complexes $[Ru(phen)_2(idpq)](ClO_4)_2$ (**1**) and $[Ru(dmp)_2(idpq)](ClO_4)_2$ (**2**) were synthesized and characterized. Cytotoxicity, apoptosis, cell cycle arrest, reactive oxygen species and mitochondrial membrane potential were assayed. The IC_{50} values of complexes **1** and **2** toward HepG-2, A549, MG-63 and HeLa cell lines range from 15.1 ± 2.1 to 24.8 ± 2.4 μM. The complexes can effectively induce apoptosis and induce cell cycle arrest at G0/G1 phase by an increase of 4.88% for **1** and 6.64% for **2** at G0/G1 phase in HeLa cells. Complexes **1** and **2** can enter the cytoplasm and accumulate in the nuclei. The complexes can enhance the level of reactive oxygen species. The ratio of the red/green is 0.74 and 0.52 for complexes **1** and **2**, which suggests that the complexes induce a decrease of mitochondrial membrane potential. These complexes induce apoptosis in HeLa through ROS-mediated mitochondrial dysfunction pathway.

1. Introduction

Since the introduction of cisplatin by Rosenberg in 1965, the area of research on bioinorganic chemistry is a challenging topic for in vivo and in vitro studies [1–4]. Platinum complexes represent one of the most successful families of clinically used anticancer drugs. However, cisplatin, a platinum(II) diamine complex used in 70% of cancer treatment has some drawbacks like toxic side-effects and lack of activity (drug resistance) against several types of cancer which are problems need to be overcome [5]. These drawbacks have motivated extensive investigations into alternative metal-based cancer therapies. In recent years, some other metals have also attracted growing research attention [6]. Among the metal-based compounds, ruthenium complex is one of the most promising potent drugs. The aqua-complex $[(\eta^6\text{-p-cymene})Ru(OH_2)(\kappa^2\text{-N,N-2-pydaT})](BF_4)_2$ (2-pydaT = 2,4-diamino-6-(2-pyridyl)-1,3,5-triazine) displays notable pH-dependent cytotoxic activity in human ovarian carcinoma cells (A2780), its IC_{50} values are 11.0 μM at pH 7.4 and 6.58 μM at pH 6.5 [7]. The monofunctional Ru(II)-arene complex $[(\eta^6\text{-arene})Ru(II)(en)Cl]^+$, where en = 1,2-diaminoethane and the arene is *para*-terphenyl exhibits promising cytotoxic effects in human tumor cells including those resistant to conventional cisplatin, and investigations have shown that the complex induces apoptosis by regulating the expression of Bcl-2 family proteins [8]. Many ruthenium(II) complexes have shown interesting properties [9–22]. $[Ru(phpy)(bpy)(dppn)]^+$ (bpy = 2,2′-bipyridine, dppn = benzo[*i*]dipyrido[3,2-*a*:2′,3′-*c*]phenazine), is 6 times more active than the platinum drug in HeLa, and the complex is able to disrupt the mitochondria membrane potential [23]. The $[Ru(phen)_2(addppn)]^{2+}$ induces apoptosis in BEL-7402 cells through ROS-mediated mitochondrial dysfunction pathway [24]. Ru(2,6-bis(2,4,6-trimethylphenyliminomethyl))(2-(phenylazo)-3-methylpyridine) shows very high cytotoxic activity against EVST-A cells with a low IC_{50} value of 0.4 μM [25]. To obtain more insight into cytotoxic activity of Ru(II) complexes, in this report, two Ru(II) polypyridyl complexes $[Ru(phen)_2(idpq)](ClO_4)_2$ (**1**) (phen = 1,10-phenanthroline, idpq = indeno [1,2-*b*]dipyrido[3,2-*f*:2′,3′-*h*]-quinoxaline-6-one) [26] and $[Ru(dmp)_2(idpq)](ClO_4)_2$ (**2**) (dmp = 2,9-dimethyl-1,10-phenanthroline, Scheme 1) were synthesized and complex **2** was characterized by elemental analysis, ES-MS and ^1H NMR. The cytotoxicity in vitro was investigated by MTT (MTT = (3-(4,5-dimethylthiazol-2-yl)-2,5-diphenyltetrazolium bromide)) assay. The apoptosis of HeLa cells induced by the Ru(II) complexes was

* Corresponding authors. Tel.: +86 20 39352122; fax: +86 20 39352129.
E-mail addresses: hhongliang@163.com (H.-L. Huang), lyjche@163.com (Y.-J. Liu).

http://dx.doi.org/10.1016/j.ica.2014.07.017
0020-1693/

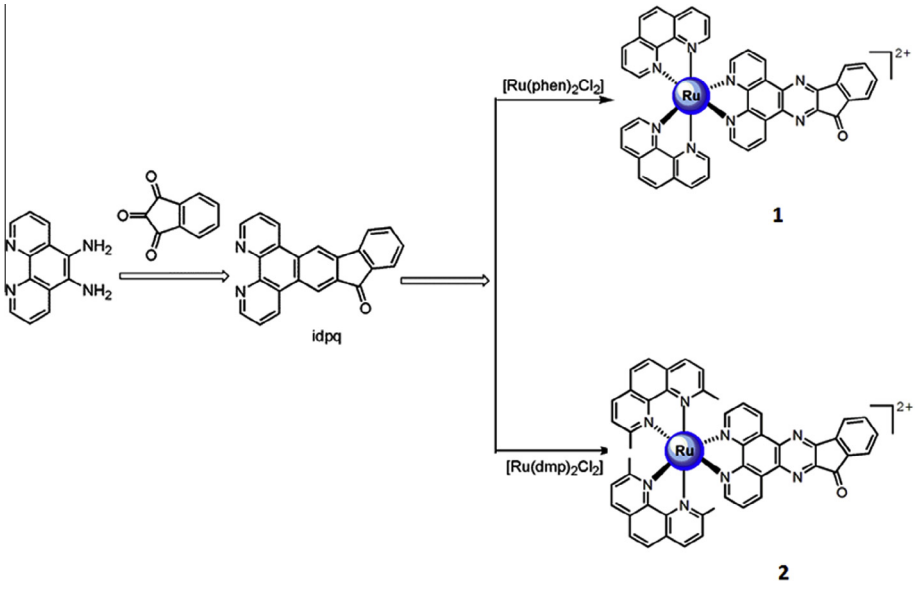

Scheme 1. The structures of complexes **1** and **2**.

studied with acridine orange (AO) and ethidium bromide (EB) staining method. The cell cycle arrest was analyzed by flow cytometry. The cellular uptake and co-localization were investigated with DAPI-stained, and the reactive oxygen species and mitochondrial membrane potential were also studied with fluorescence microscopy and microplate analyzer.

2. Experimental

2.1. Materials and method

All reagents and solvents were purchased commercially and used without further purification unless otherwise noted. Ultrapure MilliQ water was used in all experiments. DMSO and RPMI 1640 were purchased from Sigma. Cell lines of HepG-2 (Human hepatocellular carcinoma cell line), HeLa (Human cervical cancer cell line), MG-63 (Human osteosarcoma) and A549 (Human breast cancer) were purchased from the American Type Culture Collection. $RuCl_3{\cdot}3H_2O$ was purchased from the Kunming Institution of Precious Metals. 1,10-phenanthroline was obtained from the Guangzhou Chemical Reagent Factory.

Microanalyses (C, H, and N) were obtained with a Perkin–Elmer 240Q elemental analyzer. Electrospray ionization mass spectra (ES-MS) were recorded on a LCQ system (Finnigan MAT, USA) using acetonitrile as mobile phase. The spray voltage, tube lens offset, capillary voltage and capillary temperature were set at 4.50 kV, 30.00 V, 23.00 V and 200 °C, respectively, and the quoted *m*/*z* values are for the major peaks in the isotope distribution. ^{1}H NMR spectra were recorded on a Varian-500 spectrometer with DMSO [d_6] as solvent and tetramethylsilane (TMS) as an internal standard at 500 MHz at room temperature.

2.2. The preparation of ligand and complexes

The ligand ipdq and complex $[Ru(phen)_2(idpq)](ClO_4)_2$ (**1**) were synthesized according to the literature [26].

2.2.1. Preparation of $[Ru(dmp)_2(idpq)](ClO_4)_2$ (**2**)

A mixture of cis-$[Ru(dmp)_2Cl_2]{\cdot}2H_2O$ [27] (0.312 g, 0.5 mmol) and idpq (0.167 g, 0.5 mmol) in ethylene glycol (30 mL) was heated at 150 °C under argon for 8 h to give a clear red solution. Upon cooling, a red precipitate was obtained by dropwise addition of saturated aqueous $NaClO_4$ solution. The crude product was purified by column chromatography on neutral alumina with a mixture of CH_3CN–toluene (3:1, v/v) as eluent. The red band was collected. The solvent was removed under reduced pressure and a red powder was obtained. Yield: 68%. *Anal.* Calc for $C_{49}H_{34}N_8Cl_2O_9Ru$: C, 56.01; H, 3.26; N, 10.66. Found: C, 55.89; H, 3.44; N, 10.56%. ^{1}H NMR (DMSO-d_6): δ 9.49 (d, 1H, J = 7.0 Hz), 9.33 (d, 1H, J = 7.0 Hz), 8.94 (d, 2H, J = 8.5 Hz), 8.44 (d, 4H, J = 7.0 Hz), 8.27 (dd, 2H, J = 4.0, J = 4.5 Hz), 8.17 (d, 1H, J = 7.5 Hz), 8.01 (d, 2H, J = 8.5 Hz), 7.97–7.93 (m, 2H), 7.78 (d, 1H, J = 7.0 Hz), 7.69 (d, 1H, J = 6.0 Hz), 7.62 (dd, 2H, J = 5.5, J = 5.5 Hz), 7.58 (d, 1H, J = 5.5 Hz), 7.42 (dd, 2H, J = 8.5, J = 8.0 Hz), 1.95 (s, 6H), 1.79 (s, 6H). ES-MS (CH_3CN): *m*/*z* 951.4 ($[M\text{-}ClO_4]^+$), 425.6 ($[M\text{-}2ClO_4]^{2+}$).

Caution: Perchlorate salts of metal compounds with organic ligands are potentially explosive, and only small amounts of the material should be prepared and handled with great care.

2.3. Cytotoxicity assay in vitro

Standard 3-(4,5-dimethylthiazole)-2,5-diphenyltetraazolium bromide (MTT) assay procedures were used [28]. Cells were placed in 96-well microassay culture plates (8×10^3 cells per well) and grown overnight at 37 °C in a 5% CO_2 incubator. Complexes tested were then added to the wells to achieve final concentrations ranging from 10^{-6} to 10^{-4} M. Control wells were prepared by addition of culture medium (100 μL). The plates were incubated at 37 °C in a 5% CO_2 incubator for 48 h. Upon completion of the incubation, stock MTT dye solution (20 μL, 5 mg/mL^{-1}) was added to each well. After 4 h, buffer (100 μL) containing *N*,*N*-dimethylformamide (50%) and sodium dodecyl sulfate (20%) was added to solubilize the MTT formazan. The culture medium and cisplatin were used as the negative and positive controls, respectively. The optical density of each well was then measured with a microplate spectrophotometer at a wavelength of 490 nm. The IC_{50} values were determined by plotting the percentage viability versus concentration on a logarithmic graph and reading off the concentration at which 50% of cells remain viable relative to the control. Each experiment was repeated at least three times to obtain the mean values. Four different tumor cell lines were the subjects of this study: HepG-2, A549, MG-63 and HeLa cell lines.

2.4. Cellular uptake and co-localisation studies

HeLa cells were placed in 24-well microassay culture plates (4×10^4 cells per well) and grown overnight at 37 °C in a 5% CO_2 incubator. Complexes tested were then added to the wells. The plates were incubated at 37 °C in a 5% CO_2 incubator for 24 h. Upon completion of the incubation, the wells were washed three times with phosphate buffered saline (PBS). After removing the culture medium, the cells were stained with 2-(4-amidinophenyl)-6-indolecarbamidine dihydrochloride (DAPI) and visualized by fluorescence microscope.

2.5. Apoptosis assay by AO/EB staining method

HeLa cells were seeded onto chamber slides in six-well plates at a density of 2×10^5 cells per well and incubated for 24 h. The cells were cultured in RPMI 1640 supplemented with 10% of fetal bovine serum (FBS) and incubated at 37 °C and 5% CO_2. The medium was removed and replaced with medium (final DMSO concentration, 0.05% v/v) containing the complexes (25 μM) for 24 h. The medium was removed again, and the cells were washed with ice-cold PBS, and fixed with formalin (4%, w/v). Cell nuclei were counterstained with acridine orange (AO) and ethidium bromide (EB) (AO: 100 μg/mL, EB: 100 μg/mL) for 10 min. Then the cells were observed and imaged by a fluorescence microscope (Nikon, Yokohama, Japan) with excitation at 350 nm and emission at 460 nm.

2.6. Reactive oxygen species (ROS) detection

HeLa cells were seeded into six-well plates (Costar, Corning Corp, New York) at a density of 2×10^5 cells per well and incubated for 24 h. The cells were cultured in RPMI 1640 supplemented with 10% of FBS and incubated at 37 °C and 5% CO_2. The medium was removed and replaced with medium (final DMSO concentration, 0.05% v/v) containing complexes **1** and **2** (12.5 and 25 μM) for 24 h. The medium was removed again. The fluorescent dye 2′,7′-dichlorodihydrofluorescein diacetate (H_2DCFDA, 10 μM) was added to the medium to cover the cells. The treated cells were then washed with cold PBS–EDTA twice, collected by trypsinization and centrifugation at 1500 rpm for 5 min, and cell pellets were suspended in PBS–EDTA and then imaged by fluorescence microscope. The fluorescent intensity was determined by microplate analyzer (Infinite M200, TECAN, Switzerland) with excitation at 488 nm and emission at 525 nm. The fluorescent intensity was calculated by the determined fluorescent intensity minus the fluorescence intensity of the complexes in the corresponding concentration.

2.7. Mitochondrial membrane potential assay

HeLa cells were treated for 24 h with the complex in 12-well plates and were then washed three times with cold PBS. The cells were detached with trypsin–EDTA solution. Collected cells were incubated for 20 min with 1 μg/mL of JC-1 in culture medium at 37 °C in the dark. Cells were immediately centrifuged to remove the supernatant. Cell pellets were suspended in PBS and then imaged by fluorescence microscope. The fluorescent intensity was determined by microplate analyzer (Infinite M200, TECAN, Switzerland) with excitation at 488 nm and emission at 525 nm. The fluorescent intensity was calculated by the determined fluorescent intensity minus the fluorescent intensity of the complexes in the corresponding concentration.

2.8. Cell cycle arrest by flow cytometry

HeLa cells were seeded into six-well plates (Costar, Corning Corp, New York) at a density of 2×10^5 cells per well and incubated for 24 h. The cells were cultured in RPMI 1640 supplemented with FBS (10%) and incubated at 37 °C and 5% CO_2. The medium was removed and replaced with medium (final DMSO concentration, 0.05% v/v) containing complexes **1** and **2** (25 μM). After an incubation of 24 h, the cell layer was trypsinized and washed with cold PBS and fixed with 70% ethanol. Twenty μL of RNAse (0.2 mg/mL) and 20 μL of propidium iodide (0.02 mg/mL) were added to the cell suspensions and the cells were incubated at 37 °C for 30 min. Then the samples were analyzed with a FACSCalibur flow cytometry. The number of cells analyzed for each sample was 10000 [29].

2.9. Statistical analysis

All of the data were expressed as the mean ± SD. Differences between two groups were analyzed by a two-tailed Student's *t* test. Differences with $P < 0.05$ were considered statistically significant.

3. Results and discussion

3.1. Synthesis and characterization

The ligand and complex **1** were synthesized according to the literature [26]. Complex **2** was prepared by the direct reaction of ligand with $[Ru(dmp)_2Cl_2]\cdot 2H_2O$ in ethylene glycol. The desired ruthenium(II) complexes were isolated as the perchlorate and purified by column chromatography. Each synthetic step involved here is straightforward and provides a relative high yield of the desired product in pure form. In the ES-MS spectra of the complex, all of the expected signals of ($[M\text{-}ClO_4]^+$) and ($[M\text{-}2ClO_4]^{2+}$) were observed. The measured molecular weights were consistent with the expected values.

3.2. Cytotoxic activity in vitro assay

Liu reported that complex **1** interacts with CT DNA with a large DNA-binding affinity $(4.0 \pm 0.6) \times 10^6\ M^{-1}$ [26]. This prompts us to investigate the anticancer activity of the complex. The cytotoxicity of complexes **1** and **2** were comparable to that of cisplatin against HepG-2, HeLa, MG-63 and A549 cells. The IC_{50} values are listed in Table 1. Complex **1** shows more sensitive to HepG-2 cells than complex **2**. Treatment of A549 cells with **1** and **2**, the two complexes exhibit the same cytotoxic activity. However, treatment of HeLa and MG-63, complex **2** displays relatively high cytotoxic activity than complex **1** under identical conditions. Comparing the IC_{50} values, the both complexes all show lower cytotoxic effect than cisplatin and $[Ru(phen)_2(addppn)]^{2+}$ [24] on the selected cell lines. In addition, these results also suggest that different complexes reveal different cytotoxic activity against different tumor cell lines.

3.3. Apoptosis assay by AO/EB staining method

To assess whether complexes **1** and **2** cause cell death by apoptosis or necrosis, the AO/EB assays were performed. AO can pass through cell membrane, but EB cannot. As shown in Fig. 1, in the

Table 1
The IC_{50} values of complexes **1** and **2** against HepG-2, HeLa, MG-63 and A549 cell lines.

Complex	IC_{50} (μM)			
	HepG-2	HeLa	MG-63	A549
1	17.3 ± 1.5	24.8 ± 2.4	19.6 ± 2.0	15.8 ± 1.4
2	24.8 ± 2.3	15.8 ± 2.1	15.1 ± 1.8	15.8 ± 1.3
Cisplatin	11.5 ± 1.2	7.3 ± 1.4	6.6 ± 0.5	6.7 ± 0.8

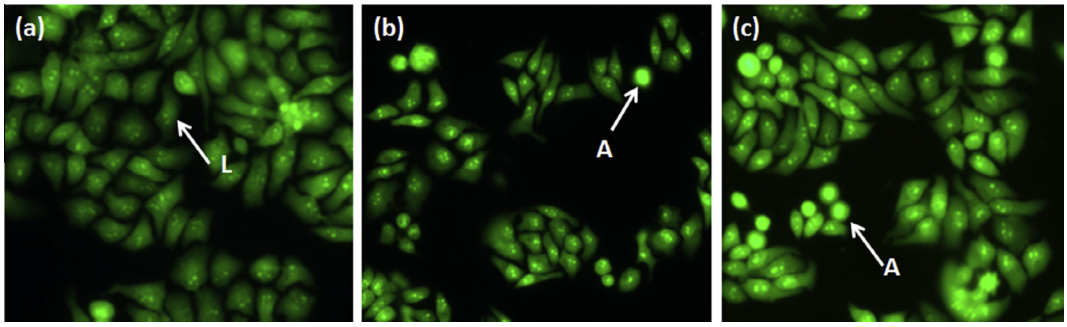

Fig. 1. AO/EB staining HeLa cells for 24 h. (a) Control, (b) and (c) treated with 25 μM of complexes **1** and **2**. L and A stand for living and apoptotic cells, respectively.

control, the living cells were stained bright green in spots (Fig. 1a) and exhibit homogeneous nuclei staining. The apoptotic and necrotic cells can be distinguished from one another using fluorescence microscopy. Treatment of HeLa cells with 25 μM of complexes **1** (Fig. 1b) or **2** (Fig. 1c) for 24 h, green apoptotic cells (typical apoptotic changes, e.g., staining bright, condensed chromatin, and fragmented nuclei) stained by acridine orange were observed. These results indicate that complexes **1** and **2** can induce apoptosis in HeLa cells.

3.4. Cellular uptake and co-localization

Most of ruthenium(II) complexes can emit fluorescence at room temperature [30–33]. Photophysical properties of complexes **1** and **2** were used to evaluate their localization in HeLa cells. Treatment of HeLa cells with complexes **1** or **2** for 24 h, the cells was stained with DAPI. As shown in Fig. 2, the blue channel shows DAPI-stained nuclei, the red channel displays the luminescence of complexes **1** and **2** with an excitation wavelength of 460 nm, and the overlay represents cellular association of the complexes. These results suggest that the complexes can be uptaken by HeLa cells and complexes can accumulate in the cell nuclei.

3.5. Reactive oxygen species (ROS) assay

To determine the effect of complexes **1** and **2** on intracellular ROS generation, HeLa cells were exposed to **1** and **2** for 24 h. ROS levels were evaluated with fluorescence microscopy using a H_2DCFDA as fluorescence probe. H_2DCFDA is a fluorescent dye that diffuses through cell membrane and is hydrolyzed by intracellular esterases to DCFH. DCFH is oxidized to DCF in the presence of ROS, DCF can emit fluorescence, and its level corresponds to the level of generated ROS [34]. As shown in Fig. 3, in the control (Fig. 3a), no fluorescence point was observed. Treatments of HeLa cells with 12.5 μM of complexes **1** (Fig. 3b) and **2** (Fig. 3c), green fluorescence points were found. In order to investigate the effect of concentration of the complexes on the fluorescent intensity, the levels of ROS were also studied with microplate analyzer. Comparing with the control, DCF fluorescent intensities increase (Fig. 4). The increasing extent of the DCF fluorescent intensity induced by **2** is higher than that induced by **1** under identical conditions. Furthermore, the levels of ROS induced by **1** and **2** are concentration-dependent. These results suggest that complexes **1** and **2** can enhance the levels of ROS.

3.6. Mitochondrial membrane potential detection

The changes in mitochondrial membrane potential ($\Delta\Psi_{MMP}$) induced by complexes **1** and **2** were assayed using JC-1 as a fluorescent probe. JC-1 with aggregates emits red fluorescence corresponding to high MMP, whereas monomeric JC-1 emits green fluorescence corresponding to low MMP. As shown in Fig. 5, in the control (Fig. 5a), the red fluorescent points were observed. After the HeLa cells were exposed to 12.5 μM of complexes **1** (5b) or **2** (5c), green fluorescent points with little red fluorescence were found. To quantitatively measure the red and green

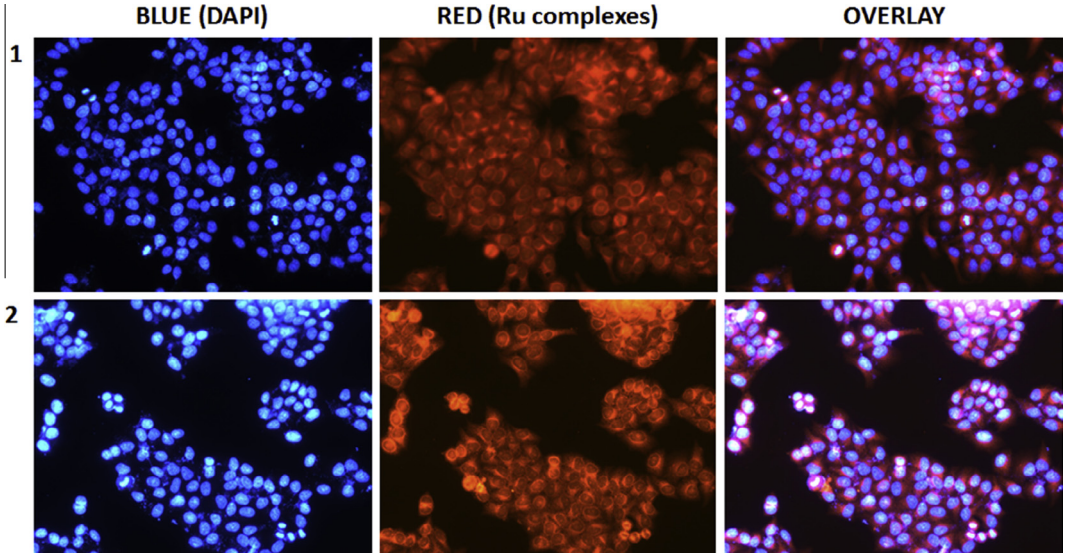

Fig. 2. Fluorescence miscroscopy images of HeLa cells exposure to 25 μM of complexes **1**, **2** for 24 h. Images show DAPI staining, cellular staining of Ru(II) complexes, and the overlay.

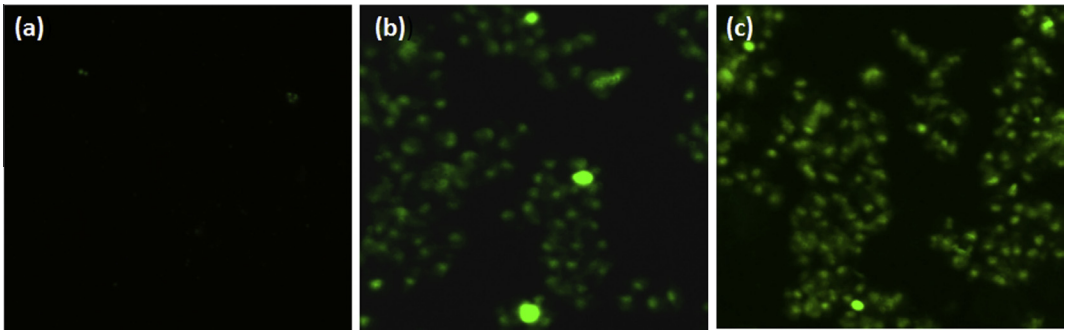

Fig. 3. Intracellular ROS was detected in HeLa cells (a) exposure to 12.5 μM of complexes **1** (b) and **2** (c) for 24 h.

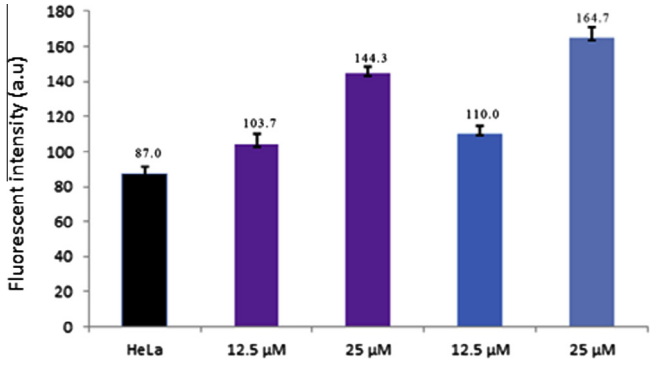

Fig. 4. Effects on ROS generation induced by different concentrations of complexes **1** (■) and **2** (■) in HeLa cells. Data were calculated from three independent experiments.

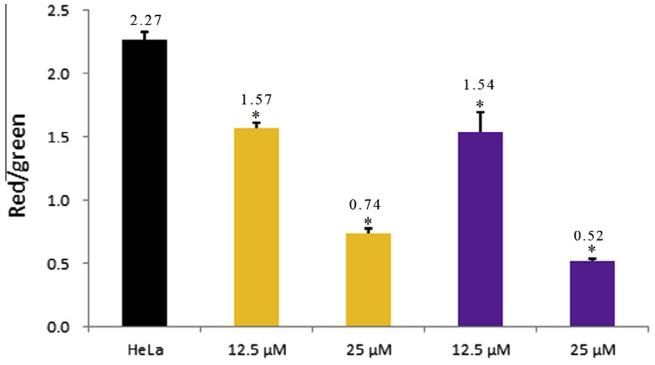

Fig. 6. Assay of HeLa cells mitochondrial membrane potential with JC-1 as fluorescent probe staining method. HeLa cells exposed to 12.5 and 25 μM of complexes **1** (■) and **2** (■) for 24 h. $^{*}p < 0.05$ represents significant differences compared with control.

fluorescent intensity, the ratios of red/green intensity were determined with microplate analyzer. In the control (Fig. 6), the ratio of red/green is 2.27. Treatment of HeLa cells with 12.5 and 25 μM of complexes **1** and **2**, the ratios of red/green are 1.57, 0.74 and 1.54, 0.52, respectively. The changes from red to green and the decrease of the ratio indicate that the complexes can induce the decrease of mitochondrial membrane. Moreover, the $\Delta\Psi_{MMP}$ shows concentration dependent manner.

3.7. Cell cycle arrest studies

The effect of complexes **1** and **2** on the cell cycle arrest of the HeLa cells was studied using flow cytometry in propidium-iodide-stained method. The status of cell cycle for cells treated with 25 μM of complexes **1** and **2** for 24 h was shown in Fig. 7, an increase of 4.88% for **1** and 6.64% for **2** of cells at G0/G1 phase was observed, accompanied by a corresponding reduction of 7.04% for **1** and 9.92% for **2** in the percentage of cells in the S phase,

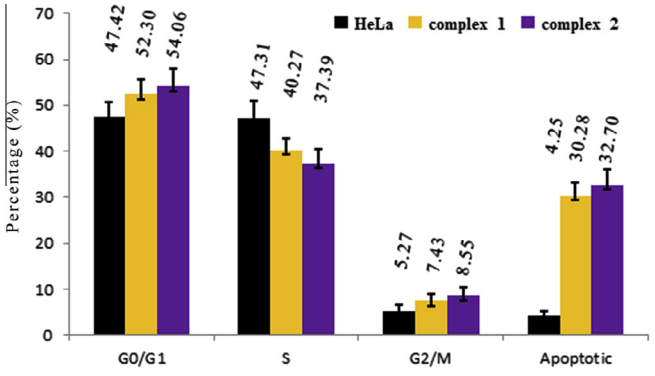

Fig. 7. Cell cycle distribution of HeLa exposure to 25 μM complexes **1** and **2** for 24 h. Data were obtained by three independent experiments.

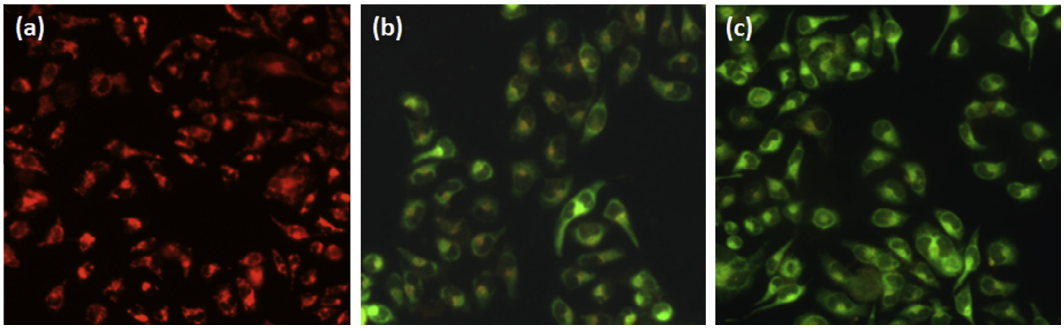

Fig. 5. Assay of HeLa cells mitochondrial membrane potential with JC-1 as fluorescent probe staining method. HeLa cells (control, a) exposed to 12.5 μM of complexes **1** (b) and **2** (c) for 24 h.

respectively. In the G2/M phase, a small amount of increase was found. These data indicate that the anti-proliferative mechanism induced by complexes **1** and **2** on HeLa cells is G0/G1 phase arrest. In addition, the apoptotic percentage in the cells increases by 26.03% for **1** and 28.45% for **2**. Obviously, complex **2** shows more effective apoptosis than complex **1** under the same conditions. This is consistent with the cytotoxic activity (IC_{50} values) of complexes **1** and **2** against HeLa cells.

4. Conclusion

Two ruthenium(II) complexes were synthesized and characterized. Complex **2** shows higher cytotoxic activity than complex **1** toward HeLa and MG-63 cells. The complexes can effectively induce apoptosis in HeLa cells. Complexes **1** and **2** can enter into the cytoplasm and accumulate in the nuclei. These complexes can enhance the levels of ROS and decrease the mitochondrial membrane potential. The complexes inhibit the HeLa cell growth at Go/G1 phase. These results exhibit that complexes **1** and **2** induce HeLa apoptosis through ROS-mediated mitochondrial dysfunction pathway.

Acknowledgments

This work was supported by the National Nature Science Foundation of China (no. 31070858), High-level Personnel Project of Guangdong Province in 2013 and the Joint Nature Science fund of the Department of Science and Technology and the First Affiliated Hospital of Guangdong Pharmaceutical University (No GYFYLH201315).

References

[1] S. Bhattacharya, S.S. Karki, R. Suresh, L. Manikandan, G.P. Senthilkumar, M. Gupta, U.K. Mazumder, R. Balaji, K. Murali, Med. Chem. Res. 20 (2011) 790.
[2] G.Y. Li, K.J. Du, J.Q. Wang, J.W. Liang, J.F. Kou, X.J. Hou, L.N. Ji, H. Chao, J. Inorg. Biochem. 119 (2013) 43.
[3] A. Castonguay, C. Doucet, M. Juhas, D. Maysinger, J. Med. Chem. 55 (2012) 8799.
[4] O. Pinato, C. Musetti, N.P. Farrell, C. Sissi, J. Inorg. Biochem. 122 (2013) 27.
[5] H.M. Pineto, J.H. Schornagel, Plenum, New York, 1996.
[6] J. Reedijk, Platinum Met. Rev. 52 (2008) 2.
[7] N. Busto, J. Valladolid, M. Martínez-Alonso, H.J. Lozano, F.A. Jalón, B.R. Manzano, A.M. Rodríguez, M.C. Carrión, T. Biver, J.M. Leal, G. Espino, Inorg. Chem. 52 (2013) 9962.
[8] A. Kisova, L. Zerzankova, A. Habtemariam, P.J. Sadler, V. Brabec, J. Kasparkova, Mol. Pharm. 8 (2011) 949.
[9] Y.Y. Xie, H.L. Huang, J.H. Yao, G.J. Lin, G.B. Jiang, Y.J. Liu, Eur. J. Med. Chem. 63 (2013) 603.
[10] N. Deepika, Y.P. Kumar, C.S. Devi, P.V. Reddy, A. Srishailam, S. Satyanarayana, J. Biol. Inorg. Chem. 18 (2013) 751.
[11] L.F. Tan, J.L. Shen, J. Liu, L.L. Zeng, L.H. Jin, C. Weng, Dalton Trans. 41 (2012) 4575.
[12] G.J. Lin, G.B. Jiang, Y.Y. Xie, H.L. Huang, Z.H. Liang, Y.J. Liu, J. Biol. Inorg. Chem. 18 (2013) 873.
[13] P. Kalaivani, R. Prabhakaran, P. Poornima, R. Huang, V. Hornebecq, F. Dallemer, V.V. Padma, K. Natarajan, RSC Adv. 3 (2013) 20363.
[14] Y.J. Liu, Z.H. Liang, H.L. Hong, Z.Z. Li, J.H. Yao, H.L. Huang, Inorg. Chim. Acta 387 (2012) 117.
[15] L.F. Tan, J. Liu, J.L. Shen, X.H. Liu, L.L. Zeng, L.H. Jin, Inorg. Chem. 51 (2012) 4417.
[16] R. Zhang, Z.Q. Ye, Y.J. Yin, G.L. Wang, D.Y. Jin, J.L. Yuan, J.A. Piper, Bioconjugate 23 (2012) 725.
[17] L. Salassa, T. Ruiu, C. Garino, A.M. Pizarro, F. Bardelli, D. Gianolio, A. Westendorf, P.J. Bednarski, C. Lamberti, R. Gobetto, P.J. Sadler, Organometallics 29 (2010) 6703.
[18] I. Bratsos, B. Serli, E. Zangrando, N. Katsaros, E. Alessio, Inorg. Chem. 46 (2007) 975.
[19] R. Pettinari, C. Pettinari, F. Marchetti, C.M. Clavel, R. Scopelliti, P.J. Dyson, Organometallics 32 (2013) 309.
[20] I.N. Stepanenko, A. Casini, F. Edafe, M.S. Novak, V.B. Arion, P.J. Dyson, M.A. Jakupec, B.K. Keppler, Inorg. Chem. 50 (2011) 12669.
[21] A. Ali, K. Saleem, D. Wesselinova, A. Haque, Med. Chem. Res. 22 (2013) 1386.
[22] A. Ali, A. Haque, K. Saleem, M.F. Hsieh, Bioorg. Med. Chem. 21 (2013) 3808.
[23] B. Peña, A. David, C. Pavani, M.S. Baptista, J.P. Pellois, C. Turro, K.R. Dunbar, Organometallics 33 (2014) 1100.
[24] G.B. Jiang, J.H. Yao, J. Wang, W. Li, B.J. Han, Y.Y. Xie, G.J. Lin, H.L. Huang, Y.J. Liu, New J Chem. 38 (2014) 2554.
[25] A. Garza-Ortiz, P.U. Maheswari, M. Siegler, A.L. Spekb, J. Reedijk, New J Chem. 37 (2013) 3450.
[26] X.W. Liu, L.C. Xu, H. Li, H. Chao, K.C. Zheng, L.N. Ji, J. Mol. Struct. 920 (2009) 163.
[27] J.P. Collin, J.P. Sauvage, Inorg. Chem. 25 (1986) 135.
[28] T. Mosmann, J. Immunol. Methods 65 (1983) 55.
[29] K.K. Lo, T.K. Lee, J.S. Lau, W.L. Poon, S.H. Cheng, Inorg. Chem. 47 (2008) 200.
[30] V. Pierroz, T. Joshi, A. Leonidova, C. Mari, J. Schur, I. Ott, L. Spiccia, S. Ferrari, G. Gasser, J. Am. Chem. Soc. 134 (2012) 20376.
[31] Y.C. Wang, C. Qian, Z.L. Peng, X.J. Hou, L.L. Wang, H. Chao, L.N. Ji, J. Inorg. Biochem. 130 (2014) 15.
[32] M. Ganeshpandian, R. Loganathan, E. Suresh, A. Riyasdeen, M.A. Akbarshad, M. Palaniandavar, Dalton Trans. 43 (2014) 1203.
[33] G.B. Jiang, Y.Y. Xie, G.J. Lin, H.L. Huang, Z.H. Liang, Y.J. Liu, J. Photochem. Photobiol. B: Biol. 129 (2013) 48.
[34] A. Kawiak, J. Zawacka-Pankau, A. Wasilewska, G. Stasilojc, J. Bigda, E. Lojkowska, J. Nat. Prod. 75 (2012) 9.